

11

Thermoelectric properties of ZnO

K. Mahmood^{1*}, M. I Arshad¹, A. Ali¹, M. Ajaz un Nabi¹, N. Amin¹, M. Azhar Khan², F. Iqbal², M. Isa³

¹Department of Physics, Government College University Faisalabad, Pakistan.

²Department of Physics, The Islamia University of Bahawalpur, Pakistan.

³Department of Physics, University of Gujrat.

*Corresponding author

Outline

Introduction.....	244
Background.....	244
Sample Preparation	245
<i>Annealing Experiment</i>	246
<i>Characterization Tools</i>	247
Principal of Seebeck Coefficient Determination	247
Effect of Annealing Temperature	247
Annealing Environment Effect	250
X-Ray Diffraction	252
Conclusion	256
References.....	256

Introduction

This chapter demonstrated the effect of annealing treatment on the thermoelectric properties of ZnO. Thin films of ZnO were grown on Silicon (100) substrate by molecular beam epitaxy using substrate temperature 430 °C and Zn-Knudsen cell temperature 289 °C. A representative sample was cut into 1cmx1cm small pieces and subjected to various annealing treatments; a set of samples was annealed in oxygen environment for one hour from 500 to 800 °C, keeping a step of 100 °C, another set of samples was annealed at 600 °C for one hour in different environment (oxygen, vacuum, zinc and successively annealed in zinc and vacuum). The Seebeck coefficient, power factor and figure of merits were calculated at room temperature. The result were showed that Seebeck coefficient and power factor increased from 222 to 1610 $\mu\text{V/K}$ and 8.8×10^{-6} to $2.6 \times 10^{-4} \text{ Wm}^{-1}\text{K}^{-2}$ as annealing temperature increased from 500 to 800 °C respectively. The Seebeck coefficient and power factor for other set of samples were also calculated and it was found that sample annealed in oxygen environment has maximum Seebeck coefficient with value 270 $\mu\text{V/K}$, while sample successively annealed in vacuum and zinc has Seebeck coefficient 95 $\mu\text{V/K}$. This observation was related with the improvement of crystal structure of grown films with annealing temperature in oxygen environment. To verified, the crystal structure, we have performed X-Ray Diffraction measurements. The XRD data demonstrated that intensity of ZnO (002) plane increased and Full Width Half Maximum (FWHM) decreased with annealing temperature, while sample annealed in oxygen environment has minimum value of FWHM and sample successively annealed in vacuum and zinc has maximum value of FWHM.

Background

The world demand for energy is increasing day by day because of huge revolution in industry and technology which consumed a bunch of energy. Oil and gas are the major sources of energy, but the prices of oil are on the rise due to limited resources of oil in world [1]. The production of toxic gases during burning of oil and gases also poses alarming challenge for environment. All these issues are driving the demand for obtaining renewable energy sources. Various renewable energy sources such as solar cells, nuclear energy, wind energy, thermoelectric generators and fuel cells have been used for energy production in the world [2-5]. Among these renewable energy sources, heat is good alternate of sustainable energy source. But it is reported by US Department of energy that more than 3000 TW of waste heat energy is lost only in US manufacturing sector per year. This huge amount of energy is equivalent to 1.72 billion barrels of oil. Therefore, thermoelectricity, direct conversion of heat into electricity, has significant potential to fulfil the increasing energy demands [6]. Furthermore, thermoelectric power generation systems generally offer low environment risk, mitigating the adverse effect of global warming, maintenance free operation, absence of toxic residuals and no moving part involved [7-10]. Thermoelectric power generation is based on the Seebeck principal which states that an emf is generated due to difference of temperature between two metallic junctions. For the conversion of heat into electricity, a thermoelectric module [Fig. 11.1] is needed. This module consists of n-type and p-type semiconductors, which are connected thermally in parallel and electrically in series. The high carrier concentration of p-type and n-type semiconductors can be achieved by doping of holes and electrons, respectively. The electrical connection between these semiconductors allows for the transfer of electrons from one semiconductor to the other, which enables the flow of current [11].

A good thermoelectric (TE) material possesses the ability to convert thermal energy into electrical energy through a process known as the Seebeck effect [12]. The efficiency of any thermoelectric material is depends upon the dimensionless quantity figure of merit and it can be written by following formula:

Figure of merit = Seebeck coefficient²*electrical conductivity/thermal conductivity

Therefore, materials with high Seebeck coefficient, high electrical conductivity and low thermal conductivity are desirable. Semiconductors are best choice for high Seebeck coefficient, high electrical conductivity and moderate thermal conductivity, so suited for thermoelectric power generation applications. Various semiconductors (GaN, InGaN, ZnO) materials are being used for thermoelectric power generation but up to date not much progress has been done in suitable material growth and energy conversion efficiency. Furthermore different strategies were also employed in the literature to enhance the figure of merit such as new compound development, adjustment of carrier concentration and nano-structuring. Annealing is prominent way to improve crystal quality, diminish intrinsic defects, enlarges grain sizes and releasing accumulated strain. Therefore, a comprehensive annealing study of ZnO would be very helpful to control the intrinsic defects density and accordingly enhanced the thermoelectric properties of ZnO thin films.

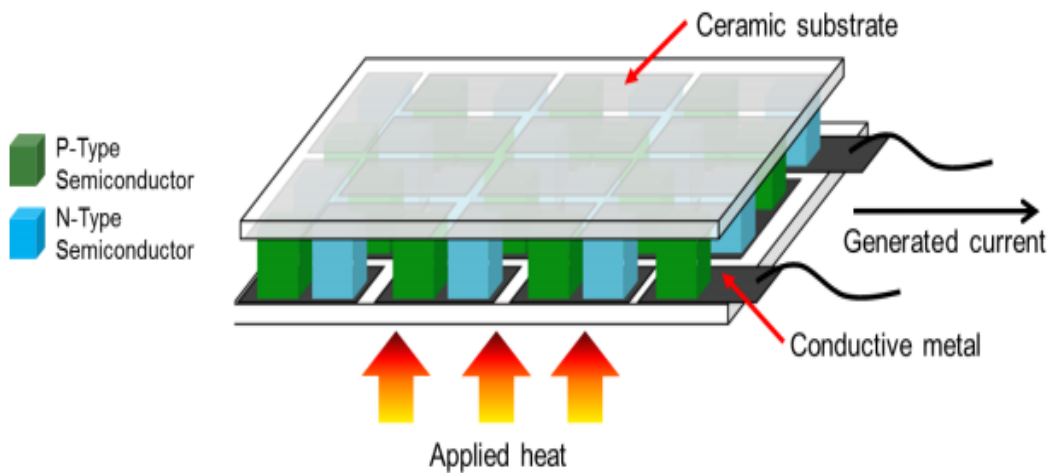


FIGURE 11.1

Common thermoelectric module consisting of different semiconductors

Sample Preparation

Molecular beam epitaxy growth techniques was used to grow the ZnO at Department of Computer and Electrical Engineering, University of North Carolina Charlotte, USA. The growth conditions for sample were set as following: substrate temperature: 430 °C, temperature of the Zn-Knudsen cell: 289°C, Zn beads purity 99.9999%, pressure of the chamber during the growth was $\sim 1 \times 10^{-4}$ mbar, growth time was 7 hours and oxygen plasma was generated by radio frequency power supply operated at 300W. The thickness of the as-grown ZnO thin film was calculated with the help of profilometer and was found to be 500nm.

Annealing Experiment

The grown ZnO thin film was cut into 1cm x 1cm pieces and subject to different annealing treatments. For annealing purposes two types of furnaces were used; tube furnace and vacuum furnace. Oxygen annealing was done using the flow of pure oxygen gas with flow rate of 50 standard cubic centimetre. To avoid the effects of impurities, flow of nitrogen was also introduced into the furnace. For annealing in vacuum environment, we have used vacuum furnace having chamber pressure 4×10^{-7} torr. This pressure was attained using rotary and diffusion pumps. When the pressure was attained, heating element was operated to gain the annealing temperature. The table 11.1 represents the annealing conditions for first group of samples annealed in oxygen environment and table 11.2 depicts the annealing conditions for 2nd batch of samples which were annealed in oxygen, vacuum, zinc and successively annealed in vacuum and zinc at 600 °C for one hour.

TABLE 11.1

Detail of annealing temperature of MBE grown ZnO on Si substrate

Annealing Environment	Annealing Temp. (°C)	Annealing Time (Mints)
Un-annealed	-	-
Oxygen	500	60
Oxygen	600	60
Oxygen	700	60
Oxygen	800	60

TABLE 11.2

Detail of MBE samples annealed in different environments

Annealing Environment	Annealing Temp. (°C)	Annealing Time (Mints)
Un-annealed	-	-
Zn-vapor	600	60
O ₂	600	60
Vacuum	600	60
Zn in Vacuum	600	60

Characterization Tools

The characterization of various annealed and as grown samples was carried out by the following equipments; the Seebeck coefficient was measured with the help of a home made Seebeck system, structural analysis was performed by X-ray diffraction having Cu- α radiation as x-ray source with wavelength 1.54 Å, Photoluminescence (Photon Systems) using laser wavelength 248 nm and Hall measurements (Ecopia 3000 Hall measurement System TM) using magnetic field 0.5T.

Principal of Seebeck Coefficient Determination

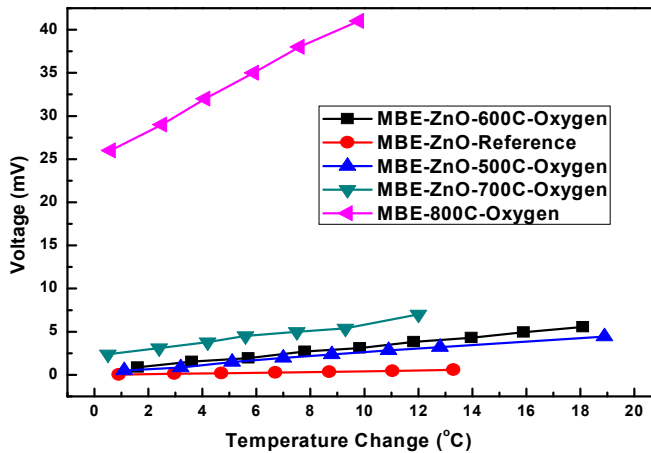
Heat moves through a solid material by means of conduction, the transfer of heat energy by microscopic diffusion and collisions of particles or quasi-particles within a body due to a temperature gradient. The rate of heat transfer per unit area through a material is the heat flux. Heat flux is directly proportional to the temperature gradient, and the constant of proportionality is the thermal conductivity of the material. There are different mechanisms which can transport heat in a material. The first is through vibrations of the internal structure of the material, such as vibrations of the crystal lattices or individual atoms. The other mechanism is through electron transport. In a material that is electrically conductive, electrons can carry heat from one end to another giving rise to the Seebeck effect. A force is needed to stop the drift and maintain equilibrium. This force takes the form of a voltage potential that develops to stop the drift of electrons, and the magnitude of this effect is quantified by the Seebeck coefficient [13]. Seebeck coefficients have units of voltage per unit temperature, usually expressed in micro-volts per Kelvin, and can be calculated using

$$S = - \frac{\Delta V}{\Delta T}$$

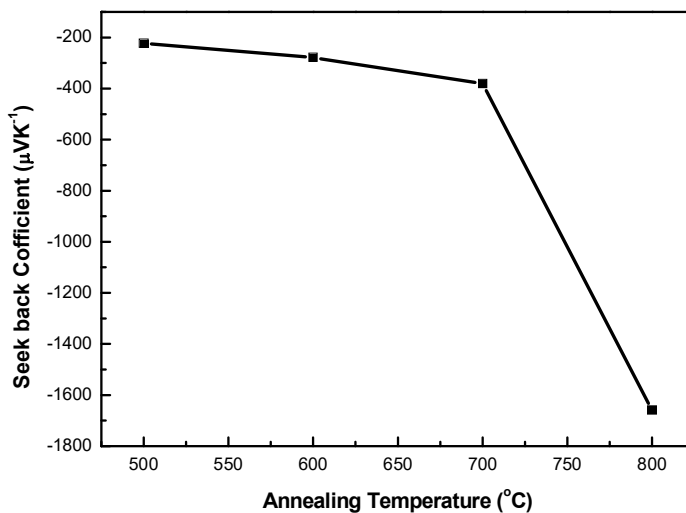
where, ΔV is the voltage difference between the hot and cold sides of a thermoelectric material and ΔT is the change in temperature between the sides. Thermocouples are often used to measure the temperatures and a voltmeter can be used to measure the voltages. The ΔV can have a positive or negative value, depending on whether the mobile charges are holes or electrons, thus giving the Seebeck coefficient a positive or negative value [14].

Effect of Annealing Temperature

Fig. 11.2 shows the temperature difference dependence of thermo-electromotive force of MBE grown ZnO annealed at different temperatures in oxygen environment for one hour. The graph demonstrates that electromotive force increases linearly as the temperature difference between cold and hot ends of sample increased. All the thermo-electromotive forces are negative which confirm that electrons are major carriers in grown samples. It is also evident from plot that induced emf increases as the annealing temperatures increases from 500-800 °C. The Seebeck coefficient was obtained by the slope of this graph and can be seen in fig. 11.3.

**FIGURE 11.2**

Graph between temperature difference and Seebeck voltage of MBE grown ZnO annealed at different temperatures in oxygen environment for one hour

**FIGURE 11.3**

Effect of annealing temperature the Seebeck coefficient of MBE grown ZnO

Fig. 11.3 demonstrated the effect of annealing temperature on the Seebeck coefficient of ZnO thin films grown on Si substrate by MBE. The Seebeck coefficient increased from 220 to 1610 $\mu\text{V}/\text{K}$ as the annealing temperature increases from 500 to 800 $^{\circ}\text{C}$. This result can be explained as: when the annealing temperature increases, the stress in the grown film decreased and crystal structure improved significantly. It is accepted fact that ZnO has high density of intrinsic defects such as oxygen vacancies and zinc interstitials [15]. These donor defects form a complex ($\text{V}_{\text{O}}\text{-Zn}_i$) which justifies the intrinsic n-type conductivity of ZnO [16, 17]. Annealing in oxygen environment fills the available oxygen vacancies and breaks the donor complex. As a result crystal structure of annealed film improved which resulted in the improvement of crystal structure. Therefore the Seebeck coefficient of annealed samples increases with annealing temperature.

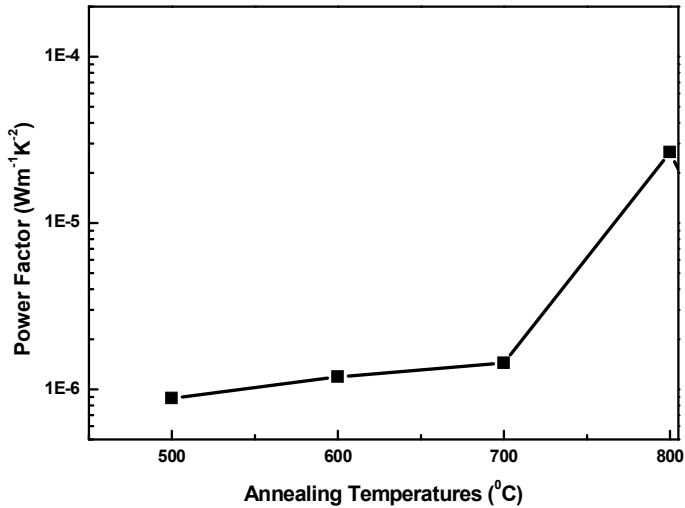


FIGURE 11.4

Effect of annealing temperature on the power factor of MBE grown ZnO

Fig. 11.4 demonstrated the effect of annealing temperature on the power factor of ZnO thin films grown on Si by MBE. The power factor increases from 8.8×10^{-6} to $2.6 \times 10^{-4} \text{ Wm}^{-1}\text{K}^{-2}$ (detail can be shown in table 11.3) as the annealing temperature increases from 500 to 800 °C.

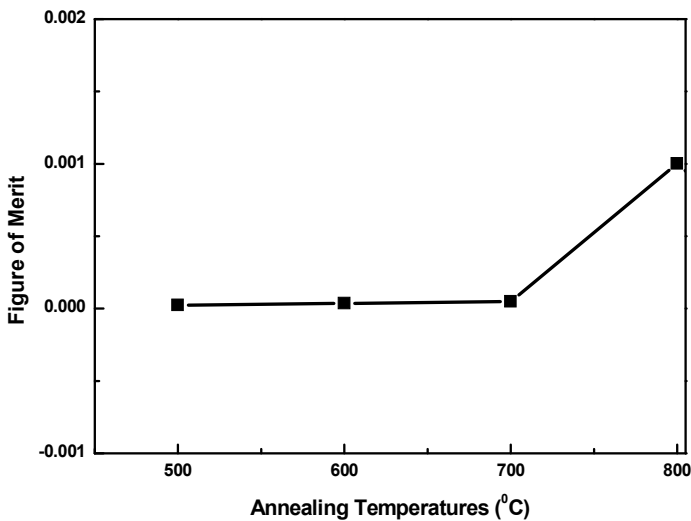


FIGURE 11.5

Effect of annealing temperature on figure of merit of MBE grown ZnO

Graph above shows the effect of annealing temperature on the dimensionless figure of merit. The dimensionless quantity, figure of merit was calculated using the following formula:

$$\text{Figure of merit} = \text{power factor} / \text{thermal conductivity}$$

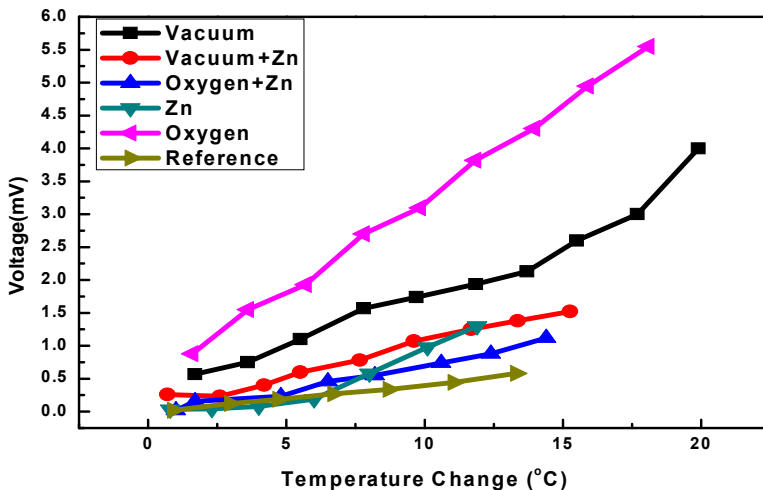
The figure of merit has increasing trend with annealing temperature [18]. It is pertinent to mention here that electrical conductivity values of 10, 9, 8 and 7 for different annealing temperatures 500, 600, 700 and 800 °C respectively, have been taken from literature.

TABLE 11.3

Effect of annealing temperature on Seebeck coefficient, power factor and figure of merit of MBE grown ZnO on Si substrate

Annealing Temperatures (°C)	Seebeck coefficient ($\mu\text{V/K}$)	Power Factor ($\text{Wm}^{-1}\text{K}^{-2}$)	Figure Of Merit
Un annealed	- 43		--
500	- 222	8.84811E -7	2.41312E-5
600	- 279	1.18841E -6	3.56524E-5
700	- 381	1.44009E -6	4.8003E-5
800	- 1660	2.66757E -5	0.001

Annealing Environment Effect

**FIGURE 11.6**

Graph between temperature difference and Seebeck voltage of MBE grown ZnO annealed in different environments for one hour at 600 °C

Fig. 11.6 shows the temperature difference dependence of thermo-electromotive force of MBE grown ZnO annealed in different environments for one hour at 600 °C. It demonstrated that electromotive force increased linearly as the temperature difference between cold and hot end of sample increased. All the thermo-electromotive forces are negative which confirm that electrons are major carriers in grown samples. The Seebeck coefficient was obtained by the slope of this graph and can be seen in fig. 11.7.

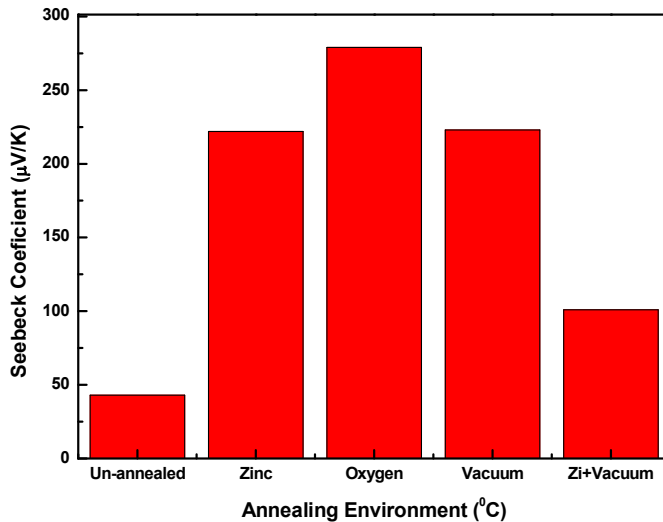


FIGURE 11.71

Effect of annealing environment on the Seebeck coefficient of MBE grown ZnO

Graph 7 explained the effect of annealing environment on the Seebeck coefficient. Sample annealed in oxygen environment has maximum value of Seebeck coefficient with value $270 \mu\text{V/K}$, while sample successively annealed in vacuum and zinc has Seebeck coefficient $95 \mu\text{V/K}$. The results are again supported the argument that improvement in crystal structure results in the enhancement of Seebeck coefficient [19]. Because annealing in oxygen would reduce the density of intrinsic defects while sample successively annealed in vacuum and zinc has high density of intrinsic defects such as oxygen vacancies and zinc interstitials defects, therefore has smallest value of Seebeck coefficient [20]. On the other hand annealing in vacuum also creates lots of oxygen vacancies and degrades the crystal structure. Therefore sample annealed in vacuum has relatively smaller value of Seebeck coefficient as compared to the sample annealed in oxygen.

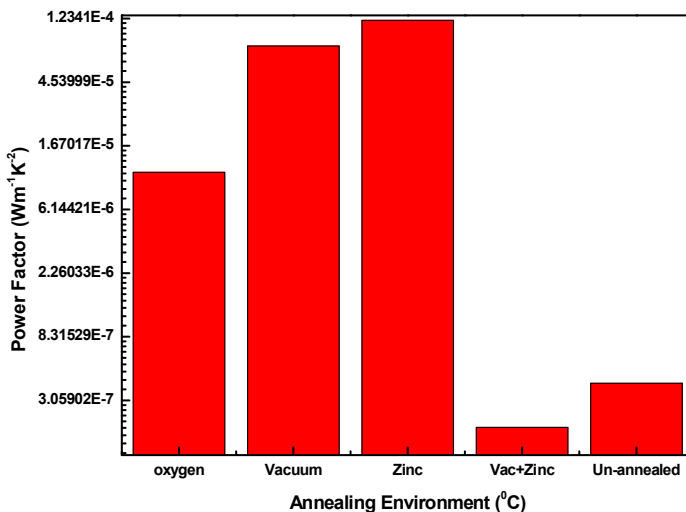


FIGURE 11.8

Effect of annealing environment on the power factor of MBE grown ZnO

Fig. 11.8 above shows the effect of annealing environment on the power factor of MBE grown ZnO on Si substrate and annealed at 600 °C for one hour. Again, the sample successively annealed in vacuum and zinc has lowest value of power factor. In conclusion, the value of Seebeck coefficient increases by improving the structure of grown films. To test the structure of annealed thin films, the XRD measurements were performed on all samples.

X-Ray Diffraction

Fig. 11.9 is the typical XRD spectrum of MBE grown samples annealed in oxygen environment for one hour at different temperatures ranging from 500 to 800 °C. The spectrum shows that all samples have two peaks at 2theta values 34.4 and 72.2° and related with ZnO (002) and (004) plane respectively [21-25]. The (002) peak in all samples is dominant which confirmed the C-axis growth of ZnO on Si substrate. The shifting of peak position is due to modulation of intrinsic defect density caused by annealing. The full Width Half Maximum of (002) peak for all samples has been calculated and shown in fig. 11.10.

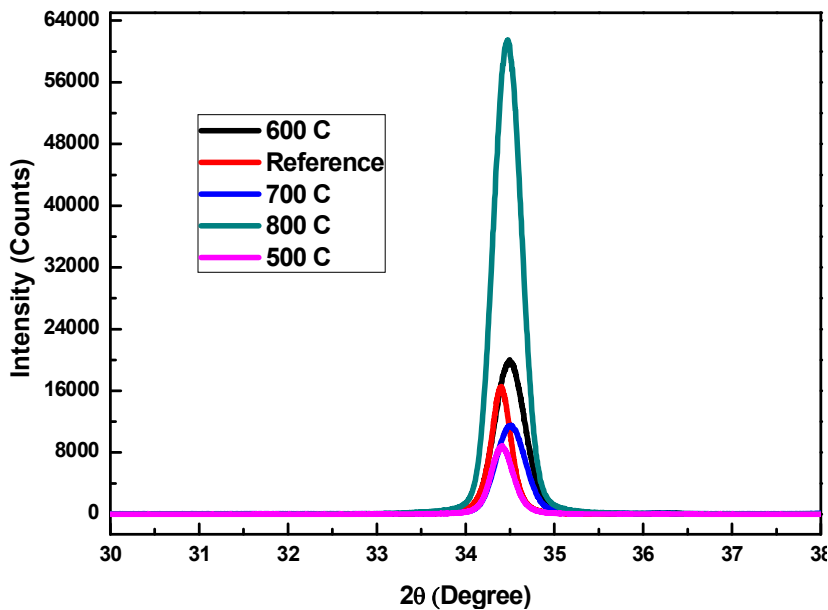


FIGURE 11.9

XRD pattern MBE grown ZnO and annealed in oxygen at various temperatures from 500-800 °C with a step of 100 °C

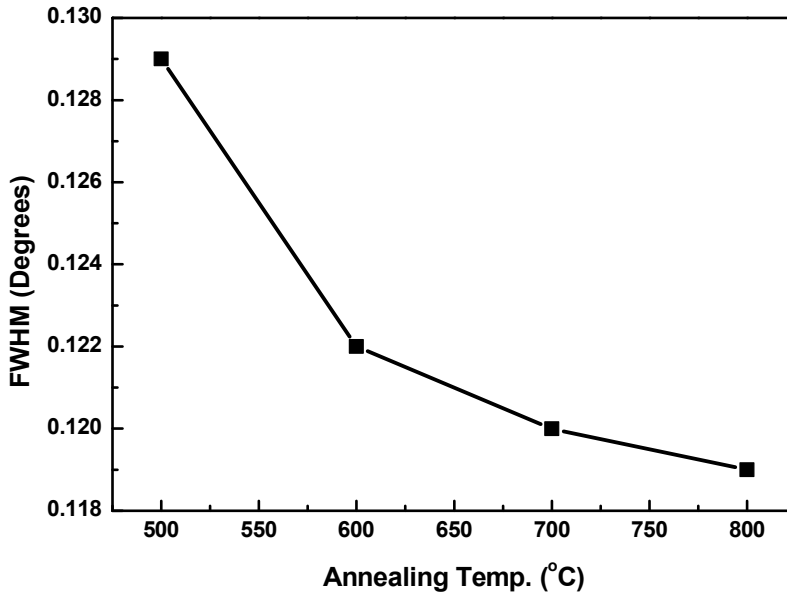


FIGURE 11.10
Relationship between annealing temperature and FWHM of ZnO (002) plane

The graph demonstrated the effect of annealing temperature on the FWHM of ZnO (002) plane. It is evident from figure that FWHM of (002) peak decreases linearly as annealing temperature increases from 500 to 800 °C. As the crystal structure of grown film directly related with the FWHM [26]. The graph showed that FWHM decreased from 0.129 to 0.119° as the annealing temperature increased from 500 to 800 °C. The decreasing trend of FWHM with annealing temperature demonstrated the improvement of crystal structure. To confirmed this argument, we have plotted the graph of crystalline size verses annealing temperature and shown in fig. 11.11. The crystalline size was calculated using Scharror's formula [27]

$$P = \lambda / \beta \cos \vartheta$$

where λ is wavelength of CuK α radiations (1.45 Å), β is Full Width at Half Maximum (FWHM).

TABLE 11.4
Effect of annealing temperature on peak position, intensity and FWHM of (002) plane

Annealing Temp. °C	(002) Peak Position (2 θ)	(002) peak Intensity (Counts)	FWHM (Degree)
Reference	34.40	16560	0.407
500	34.40	8669	0.403
600	34.90	20035	0.392
700	34.51	11525	0.387
800	34.47	61489	0.370

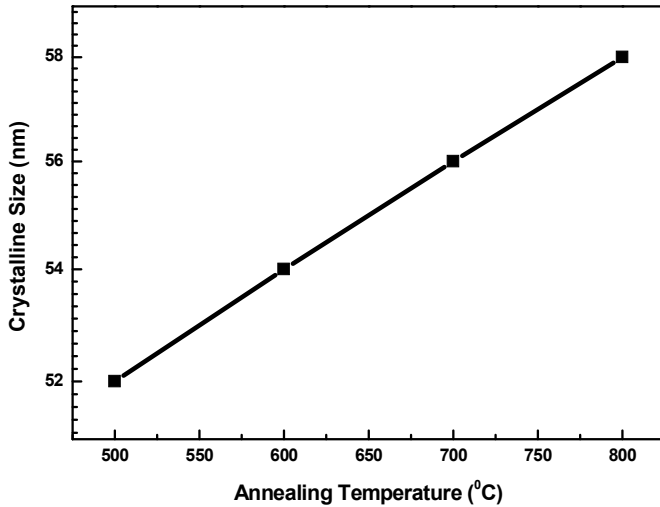


FIGURE 11.11

Effect of annealing temperature on crystalline size of MBE grown ZnO thin films

The figure 11.11 above demonstrated the effect of annealing temperature on the crystalline size of MBE grown ZnO thin films on Si substrate. The crystalline size increased from 52 nm to 58 nm as the annealing temperature increased from 500 to 800 °C. It is reported in literature that crystalline size is directly related with the crystal structure of grown films. Therefore we argued that the crystal structure of annealed thin films improve significantly with annealing temperature.

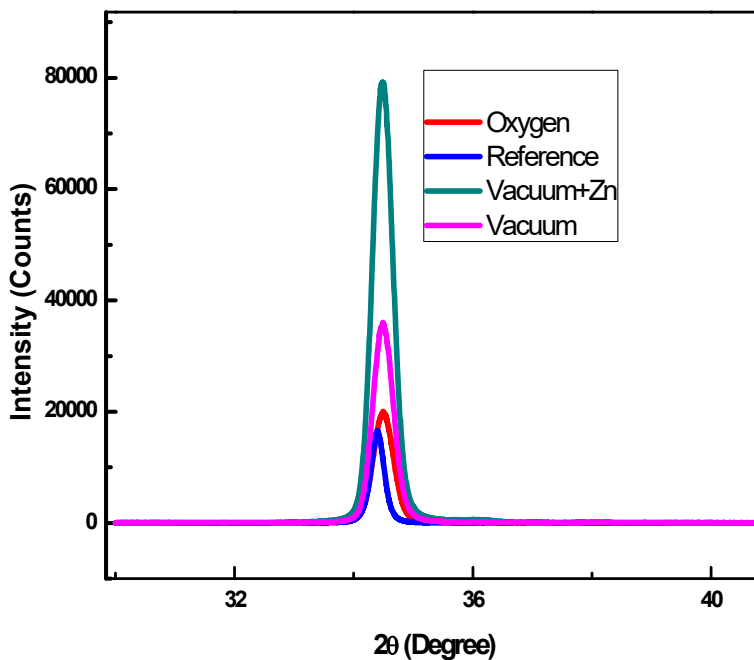


FIGURE 11.12

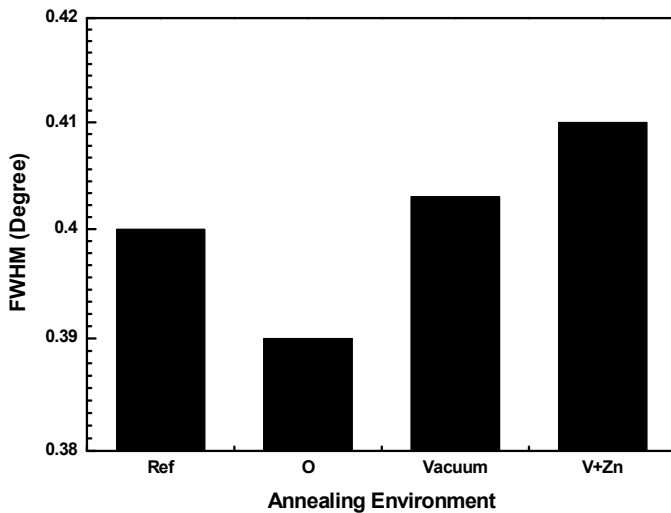
Typical XRD spectrum of ZnO thin films grown by MBE and annealed in different environments for one hour

Fig. 11.12 is the typical XRD spectrum of MBE grown samples annealed in different environments for one hour at 600 °C. The spectrum shows that all samples have one peak at 2theta values 34.4 and related with ZnO (002) plane. The (002) peak in all samples is dominant which confirmed the C-axis growth of ZnO on Si substrate [28]. The full Width Half Maximum of (002) peak for all samples has been calculated and shown in fig. 11.13 and table 11.5.

TABLE 11.5

Effect of annealing environment on peak position, intensity and FWHM of (002) plane

Annealing Environment	(002) Peak Position (2θ)	(002) peak Intensity (Counts)	FWHM (Degree)
Reference	34.40	16560	0.407
Oxygen	34.90	20035	0.392
Vacuum+Zn	34.48	79282	0.393
Vacuum	34.48	36072	0.402

**FIGURE 11.13**

Effect of annealing environment of FWHM of MBE grown thin films on Si substrate

Fig. 11.13 above displayed the effect of annealing environment on the FWHM of ZnO (002) plane. The annealed in oxygen environment has smallest value of FWHM, while sample successively annealed in vacuum and zinc has largest value of FWHM. This result can be explained as; annealing in oxygen results in the reduction of defect density in the sample [29]. But sample successively annealed in vacuum and zinc would have large density of intrinsic defects like oxygen vacancies and zinc interstitials. Therefore decrease of FWHM while annealing in oxygen and increase of FWHM while successively annealing in vacuum and zinc is justified.

Conclusion

In this study, we have demonstrated the effect of annealing treatment the thermoelectric properties of MBE grown ZnO on Si substrate. The thermoelectric properties of as grown sample were enhanced by annealing the samples in various annealing environments. It was observed that Seebeck coefficient and power factor were significantly improved by annealing in oxygen environment and further increased by increasing the annealing temperature from 500-800 °C. We argued that enhancement in thermoelectric properties is linked with improvement in the structure of annealed films. The structure of annealed films was verified using X-Ray Diffraction analysis. XRD measurements showed that intensity of ZnO (002) plane increased and Full Width Half Maximum (FWHM) decreased with annealing temperature, while sample annealed in oxygen environment has minimum value of FWHM and sample successively annealed in vacuum and zinc has maximum value of FWHM.

References

1. Weibao Guan, Liying Zhang, Chao Wang, Yuanxu Wang, *Mat. Sci. Semi. Proc.* 66 (2017) 247.
2. Ehsanul Kabir, Pawan Kumar, Sandeep Kumar, Adedeji . Adelodun, Ki-Hyun Kim, *renewable and Sustainable energy reviews*, 82 (2018) 894.
3. B. K Sahu, *renewable and Sustainable energy reviews*, 81 (2018) 1393.
4. S. Kosai, H. Unesaki, *Applied Energy*.
5. Yuichi Michiue, Hitoshi Nishijima, Yoshikazu Suzuki, Takao Mori, *Solid State Science*, 65 (2017) 29.
6. Corson L. Cramer, Jesus Gonzalez-Julian, Paul S. Colasuonno, Troy B. Holland, *Journal of European Ceramic Society*, 37 (2017) 4693.
7. Seyed Ali Ghahari, Ehsan Ghafari, Na Lu, *Construction and building materials* 146 (2017) 755.
8. Shiyang Liu, Sunjuan Peng, Jun Ma, Guojian Li, Xuesi Qin, Mengmeng Li, Qiang Wang, *Superlattices and microstructures*, 104 (2017) 282.
9. Lihong Shi, Jie Chen, Gang Zhang, Baowen Li, *Phys. Lett. A*, 376 (2012) 978.
10. Seung-Hwan Lee, Jung-Hoon Lee, Seong-Jin Choi, Jin-Seong Park, *Ceramic International*, 43 (2017) 7784.
11. K. P. Ong, D. J. Sing, P. Wu, *Phys. Review* 83 (2011) 115110.
12. A. Shakour, *Annu. Rev. Mater. Res.* 41 (2011) 399.
13. A V Dmitriev, I P Zvyagin, *Current trend in the physics of thermoelectric materials. Physics-Uspekhi* 53 (2010) 789.
14. A. Shakouri, *Annu Rev. Mater. Res* 4, 339- 431 (2011).
15. A.V. Dmitriev, I. P. Zvyagin, *Physics- Uspekhi* 53(8), 789 -803 (2010).
16. T. Teranishi, Y. Mori, H. Hayashi, A. Kishimoto, *J. Am. Ceram. Soc.* 92, 690 (2012) .
17. Y. Tanaka, T. I. Fuku, K. Tsuchida, A. Kato, *J. Mater. Sci. Lett.* 16, 155 (1997).
18. K. H. Kim, S. H. Shim, K. B. Shim, *J. Am. Ceram. Soc.* 88, 628 (2005).
19. Y. Fujishiro, M. Miyata, M. Awano, K. Maeda, *J. Am. Ceram. Soc.* 87, 1890 (2004).
20. L. Li, L. Fang, X. J. Zhou, L. Zhao, S. Jiang, *Journal of Electron Spectroscopy and Related Phenomena* 173, 7-11 (2009).
21. C. Bera, M. Soulier, C. Navone, G. Roux, J. Simon, S. Volz, N. Mingo, *J. Appl. Phys.* 108, 124306 (2010).

22. Aparna Thankappana, Divya S, Sheenu Thomas, V.P.N. Nampoori, *Optics & Laser Technology* 52 (2013) 37–42.
23. Shaivalini Singha, P. Chakrabarti, *Superlattices and Microstructures* 64 (2013) 283–293.
24. K. Sowri Babu, A. Ramachandra Reddy, Ch. Sujatha, K.V.G. Reddy, A.N. Mallika, *Materials Letters* 110 (2013) 10–12.
25. C.Y. Wang, S.Y. Maa, F.M. Li, Y. Chen, X.L. Xu, T. Wang, F.C. Yang, Q. Zhao, J. Liu, X.L. Zhang, X.B. Li, X.H. Yang, J. Zhu, *Materials Science in Semiconductor Processing* 17 (2014) 27–32.
26. M. Asghar, K. Mahmood, M-A Hasan, *Key Engineering Material*. 512 (2012) 132.
27. Vrushali Shelke, M.P. Bhole, D.S. Patil, *Materials Chemistry and Physics* 141 (2013) 81e88.
28. Chenghua Sui, Zhong Lu, Tianning X, *Optical Materials* 35 (2013) 2649–2653.
29. M. Asghar, K. Mahmood, I. T Ferguson, M Yasin Raja, Y-H Xie, R. Tsu, M-A Hasan, *Semicond. Sci. Technol.* 28 (2013) 105019.